Low-Loss Guiding Structures for THz Frequency Applications

A. G. Engel, Jr., T. E. van Deventer and Linda P. B. Katehi

NASA Center for Space Terahertz Technology
The University of Michigan

Abstract — The design and construction of low-loss monolithic transmission lines are critical to systems which require that THz-power be guided to the antenna front-end. This paper proposes two types of novel monolithic guiding structures, which are designed for the 0.4–2.0 THz and 0.1–0.4 THz ranges, respectively. Propagation in each of the waveguides is characterized by applying a mode-matching technique, and the structures are predicted to exhibit excellent power confinement and low losses. A modified integral equation method for the efficient and accurate analysis of three-dimensional structures such as power dividers, bends and stubs is also presented.

1 Introduction

Technology based on the frequency range of 0.1–2.0 THz offers narrow-beam, high-resolution antennas which are essential for intelligent computer control guidance, command systems for space applications, and sensors which operate in optically opaque media. Since these systems require that the generated THz-power be guided to the antenna front-end through complex feeding networks, the design and construction of low-loss monolithic transmission lines are critical.

There are two typical approaches for the design of these transmission lines. The first approach extends the use of planar conductors in well-established monolithic millimeter wave technology to higher frequencies. Planar circuit elements such as loads, transitions, junctions and lines perform quite well at frequencies up to 100 GHz, but ohmic and radiation losses become unacceptably high as the frequency increases further. The second approach extends optical techniques to lower frequencies. This approach is hindered by three factors. First, optical materials are usually incompatible with the semiconducting materials which are needed for active devices. Second, phenomena which dominate optical waves, such as nonlinear wave characteristics, are not present at terahertz frequencies. Finally, phenomena which are ignored at optical frequencies, such as radiation and electromagnetic coupling, are not negligible at terahertz frequencies.

A novel approach for the design of two types of monolithic guiding structures is presented in this paper. The two types are designed for specific frequencies in the 0.4–2.0 THz and 0.1–0.4 THz ranges, respectively. The development of these structures consists of two steps. The first step employs a well-known mode-matching technique to design and analyze propagation in two-dimensional structures. The second step considers the problem of circuit element design, and a modified integral equation technique is presented for the analysis of three-dimensional structures such as power dividers, bends and stubs.

2 Design

The design of the new waveguides is based on the millimeter wave dielectric waveguides which were extensively investigated for hybrid circuit applications in the 1970's and early 1980's. Examples of these waveguides include dielectric image guides [3], strip dielectric guides, insulated image guides, strip-slab guides [4], inverted strip dielectric guides [6], cladded image guides [5], and trapped image guides [7]. Like the mm-wave dielectric guides, the new waveguides are constructed from combinations of layers and ridges of various permittivities in order to provide a region wherein the propagating power is well-confined. However, whereas the widths of the mm-wave guides approach one guided wavelength in order to maximize field confinement, the dimensions of the new waveguides are on the order of a fraction of a guided wavelength, so that passive circuit elements such as inductors and couplers may be developed from these structures. In addition, the new waveguides are constructed from dielectric materials and structures which are available in monolithic technology so that the integration of active devices is possible. Also, the proposed structures may be applied as low-loss feeding networks and highly efficient radiating elements for arrays, since the physical size and dominant field component are similar to those of conventional microstrip.

The proposed structures consist of alternating layers of high and low permittivities (Figure 1). The abrupt changes in the permittivities in the x-direction are designed to optimize power confinement in the layer with the lowest permittivity. This layer, designated the *propagation layer*, is away from the ground plane, resulting in minimal ground plane conductor loss. A ridge or a semi-embedded strip provides power confinement in the y-direction. Two types of construction are proposed.

The first type of structure is suitable for the 0.4–2.0 THz region. The structures may be either ridged or semi-embedded and will be made of semiconducting materials grown on GaAs or InP substrates. The ridged structure is created by etching a layered wafer. The semi-embedded waveguide is fabricated by etching

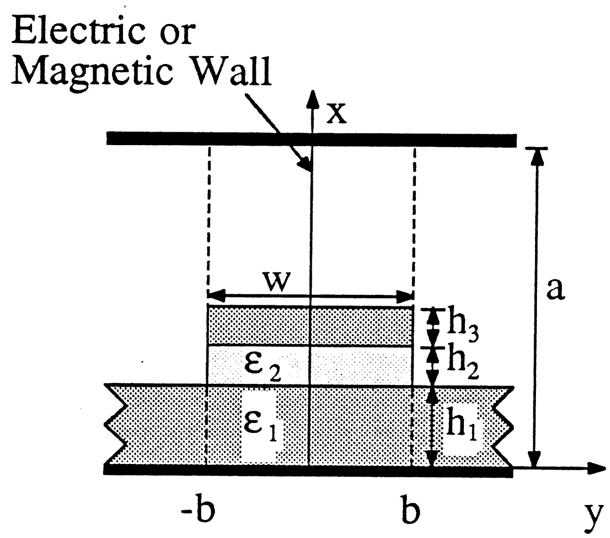

Figure 1: General structure for mode matching analysis.

a well of appropriate dimensions into a semiconducting substrate, filling the well with layers of intrinsic semiconducting materials using regrowth techniques, and etching again. In both the ridged and the semi-embedded structures, layers of 5–10 microns are required, and these layers can be grown by MOCVD.

As the frequency of operation decreases, thicker layers are required and the times required to grow the layers on the wafers become impractically large. Hence, a second type of waveguide is proposed for the sub-mm wave region (0.1–0.4 THz). This structure is constructed from a combination of semiconducting substrates and dielectric films; for example, a wafer of GaAs may be covered with a polyamide film, attached to another GaAs wafer with a thin epoxy glue, and etched to produce a ridged waveguide. The epoxy is expected to create a gap of approximately 1 micron, which would not affect the propagation characteristics. A similar structure could be created with silicon wafers and a quartz film; in this case, the wafers are attached with electrobonding.

In both cases, the waveguide construction fosters straightforward integrated circuit fabrication. Active devices may be fabricated on the substrates prior to the creation of the actual guiding structures. Transitions from the waveguides to the active devices could consist of very short lengths of microstrip near the devices. Passive structures may be created by fabricating the transmission lines in the desired pattern on the substrate.

3 Characterization of Two-Dimensional Structures

The propagation constants γ $(=\alpha + j\beta)$ and fields of the proposed lines have been analyzed using a mode-matching method, similar to the ones employed in [1, 2, 3, 8, 9, 10]. The general structure, shown in Figure 1, is uniform in the z-direction. Along the y-axis, the structure is divided into sections at $y = \pm b$. Each section is divided into layers along the x-axis at $x = h_1$, $h_1 + h_2$ and $h_1 + h_2 + h_3$. Each layer is characterized by its permittivity ϵ; losses are accounted for with a complex permittivity $\epsilon = \epsilon_o \epsilon'(1.0 - j\tan\delta)$. The outer sections ($|y| > b$) extend to $y = \pm\infty$, and the ceiling is chosen to be far enough away from the guiding structure so as to not affect the guidance properties. Using symmetry, the structure can be simplified by adding either a magnetic or electric wall in the middle and only considering half of the structure.

Each section of the structure is a section of an inhomogeneous parallel plate waveguide, which supports TE_x and TM_x modes. The boundary conditions at $x = a_i$ determine the x-dependence of each mode in each section. Mode matching is utilized at $y = -b$, giving a matrix equation which relates the mode amplitudes in the section $y < -b$ to the mode amplitudes in the section $-b < y < 0$. A homogeneous system of equations results from the boundary conditions at $y = 0$. Values for the propagation constant are ascertained from zeros of the determinant of the system, and the homogeneous system may then be solved for the mode amplitudes.

The design parameters of an example of each type of guiding structure are given in Table 1 and the characterization of these structures is shown in Figures 2–7. The results were obtained using 18 TE_x and 18 TM_x modes in each section. The structures are designed specifically for 0.650 and 0.250 THz, respectively. Each structure has a GaAs substrate with a ground plane; the 0.650 THz waveguide consists of layers of AlAs and GaAs, and the 0.250 THz waveguide consists of layers of polyamide and GaAs. The dimensions of the propagation layers at the design frequencies are on the order of 1/10th of a guided wavelength $\lambda_g (= 2\pi/\beta)$.

Plots of the phase constant versus frequency for the dominant and first higher order modes of the 0.650 THz structure are shown in Figure 2. The dominant mode has no cut-off frequency, while the first higher order mode cuts off at approximately 1.250 THz. Similar results hold for the 0.250 THz structure (Figure 5), where the first higher order mode cuts off at 0.480 THz.

Both the dominant and first higher order modes are TM_z-like modes, with dominant electric field components in the x-direction. The dominant mode is very

0.650THz Waveguide	0.250THz Waveguide
$h_1 = 0.036\lambda_g$ (13μm)	$h_1 = 0.032\lambda_g$ (32μm)
$h_2 = 0.048\lambda_g$ (17μm)	$h_2 = 0.049\lambda_g$ (49μm)
$h_3 = 0.122\lambda_g$ (43μm)	$h_3 = 0.116\lambda_g$ (116μm)
$w = 0.064\lambda_g$ (23μm)	$w = 0.091\lambda_g$ (90μm)
$\epsilon_1 = 12.85\epsilon_o$ (GaAs)	$\epsilon_1 = 12.85\epsilon_o$ (GaAs)
$\epsilon_2 = 10.0\epsilon_o$ (AlAs)	$\epsilon_2 = 3.0\epsilon_o$ (polyamide)

Table 1: Parameters (as described in Figure 1) for waveguide design examples.

similar to a typical microstrip mode, so that the aforementioned coupling to active devices via short lengths of microstrip is easily achievable.

The power density of the dominant mode of each waveguide is extremely well-confined in the respective propagation layers (Figures 4 and 7). The power is better concentrated in the propagation layer in the latter example due to the larger contrasts between permittivities in adjacent layers. The power confinement is expected to lead to low radiation losses at discontinuities.

After including losses in the dielectric layers, the attenuation constant α of the dominant mode of each structure was calculated as a function of frequency (Figures 3 and 6). Approximate attenuation constant values for the two examples are 0.19 dB/λ_g (400 dB/m) at 0.650 THz and 0.05 dB/λ_g (18 dB/m) at 0.250 THz, respectively. When the lossless and lossy cases are compared, the phase constants β do not differ significantly. The attenuation of the waveguides is also contrasted with the attenuation of the conventional rectangular waveguide and microstrip. The rectangular waveguides were designed with center frequencies comparable to the design frequencies of the monolithic waveguide examples, and the attenuation of the rectangular waveguides from sidewall conductor losses was calculated in accordance with [11]. The microstrip attenuation from both conductor and dielectric losses was calculated using the technique described in [12]. Due to the impracticality of microstrip at 0.650 THz, the microstrip is shown only in com-

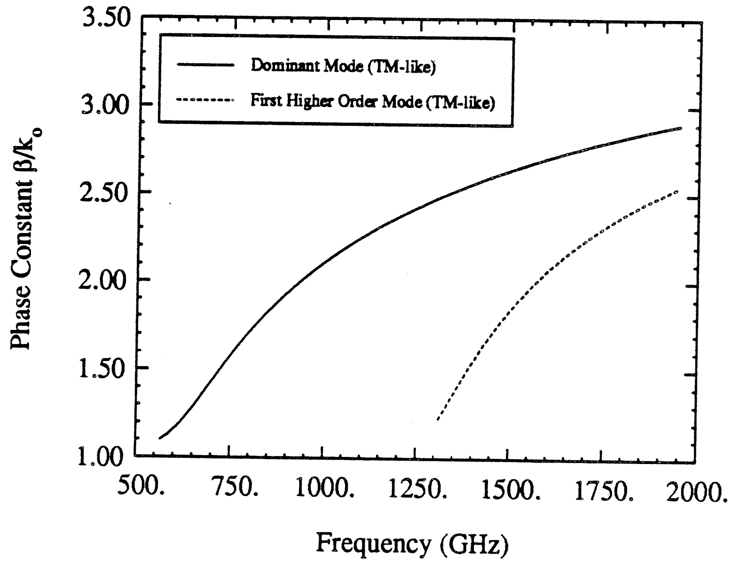

Figure 2: Phase constant of the 0.650 THz waveguide (Table 1).

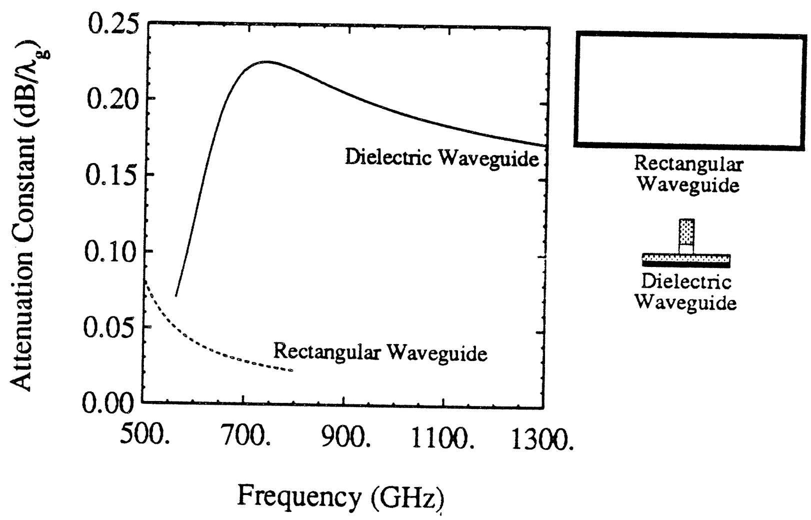

Figure 3: Attenuation constant of the 0.650 THz waveguide (Table 1, with $\epsilon_1 = 12.85(1.0 - j0.004)$ (GaAs) and $\epsilon_2 = 10.0(1.0 - j0.004)$ (AlAs)). Also shown is the attenuation of a 0.0367cm by 0.0184cm rectangular waveguide with gold sidewalls (conductivity = 4.1 x 10^5 S/cm). The two guiding structures are drawn in the same scale.

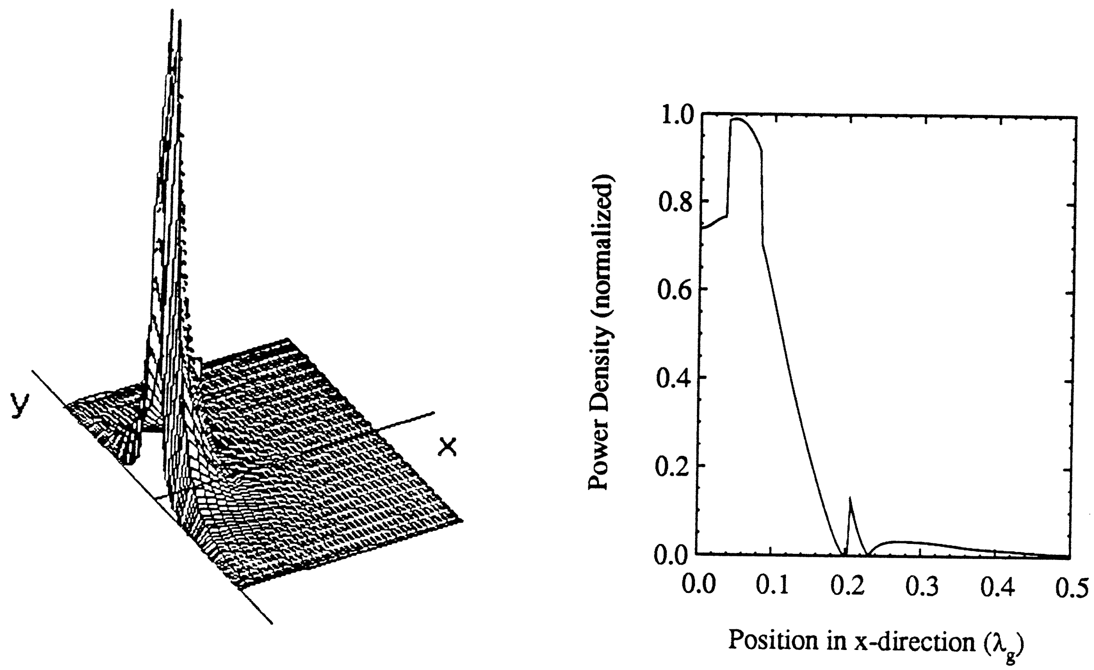

Figure 4: Power density in the 0.650 THz structure: At left, over the cross-section of the waveguide; at right, along the centerline of the waveguide.

parison to the 0.250 THz example. Although the new guiding structures do not have the extremely low attenuation exhibited by the rectangular waveguides, the new waveguides are smaller, and their monolithic nature allows for both easier construction of passive circuit elements (such as couplers, stubs, T-junctions, and inductors) and less arduous integration of active devices and device–waveguide transitions.

4 Characterization of Three-Dimensional Structures

The design of circuit elements requires a rigorous theoretical characterization of three-dimensional structures. Theoretical studies on geometrically simple optical and microwave dielectric waveguides have been presented in the past decade using approximate or numerical methods, such as the mode-matching technique described in the previous section. These methods have been exclusively applied to two-dimensional problems. Most of the existing numerical techniques perform a fine discretization of the cross-section introducing many unknowns and strong numerical instabilities. Consequently, an extension of these methods to three-dimensional problems introduces many practical limitations and requires special care [13].

Therefore, a novel method was developed to calculate the propagation characteristics of dielectric ridge structures in high frequency monolithic integrated

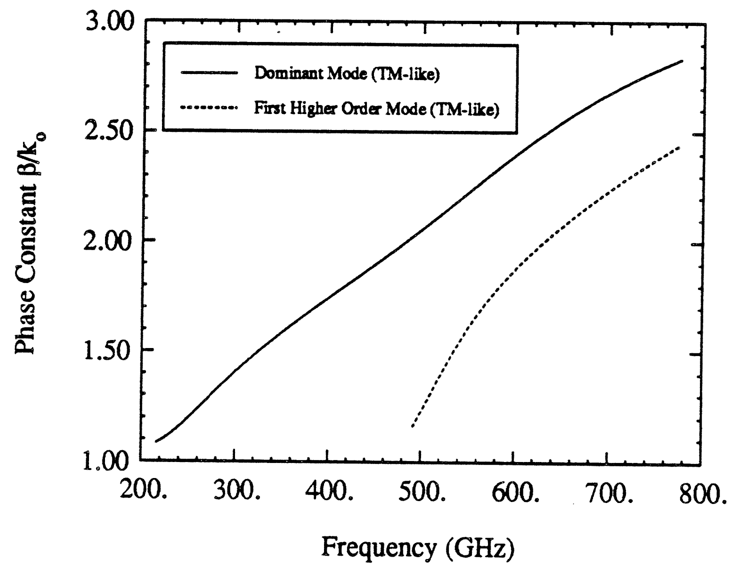

Figure 5: Phase constant of the 0.250 THz waveguide (Table 1).

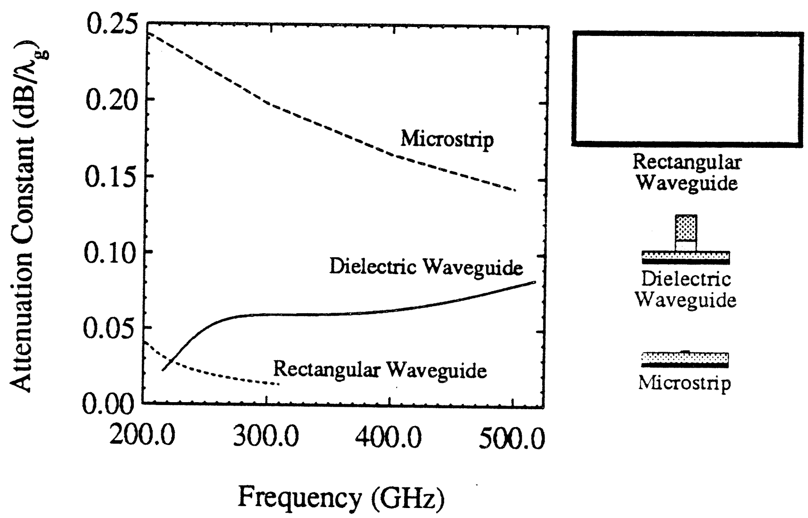

Figure 6: Attenuation constant of the 0.250 THz waveguide (Table 1, with $\epsilon_1 = 12.85(1.0 - j0.002)$ (GaAs) and $\epsilon_2 = 10.0(1.0 - j0.001)$ (polyamide)). Also shown is the attenuation of a 0.0955cm by 0.0478cm rectangular waveguide with gold sidewalls; and a 50Ω microstrip with substrate height = 100μm, strip width = 75μm, GaAs substrate ($\epsilon_r = 12.85(1.0 - j0.002)$), and strip conductivity = 3.33 x 10^5 S/cm. The three guiding structures are drawn in the same scale.

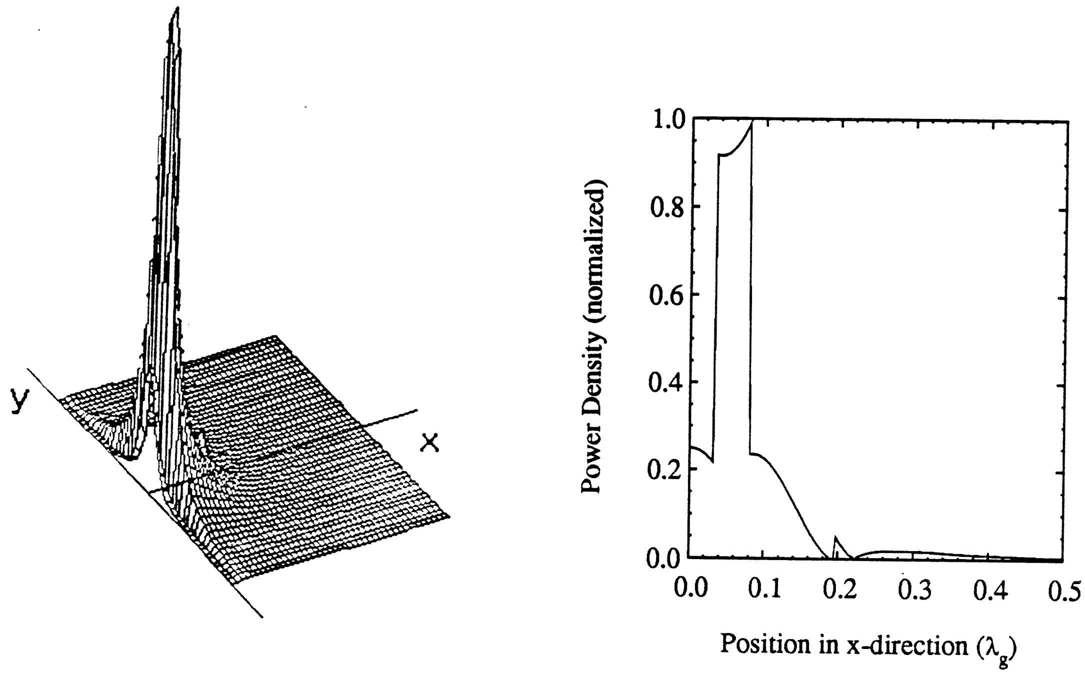

Figure 7: Power density in the 0.250 THz structure: At left, over the cross-section of the waveguide; at right, along the centerline of the waveguide.

circuits. The modified planar integral equation approach discussed here is a two-dimensional methodology which is rather unique in terms of combined accuracy and simplicity and has demonstrated excellent performance when applied to basic dielectric structures. The major advantage of this technique is that it can easily be extended to three dimensional problems without increasing the complexity of the solution.

For the sake of simplicity in the presentation of the technique and without loss of generality, we consider the dielectric structure shown in Figure 8 with non-magnetic materials and with the thickness $2h$ equal to a fraction of the dielectric wavelength and small compared to the strip width. Under these assumptions, the material of region (3) may be represented by an equivalent electric polarization current distribution occupying volume V_3. This volume polarization current is then replaced with an equivalent planar current sheet extending over the surface S_e. The equivalent surface current density radiates an electromagnetic field given by the well-known Pocklington integral equation involving the dyadic Green's function for the problem. In order to make the two boundary value problems presented in Figure 8 equivalent, the radiated field has to be identical to the original field on the surface S_3 surrounding volume V_3. Appropriate generalized boundary conditions are then enforced at the strip surfaces which provide a modified integral equation.

As a demonstration of the validity of the presented technique, the phase con-

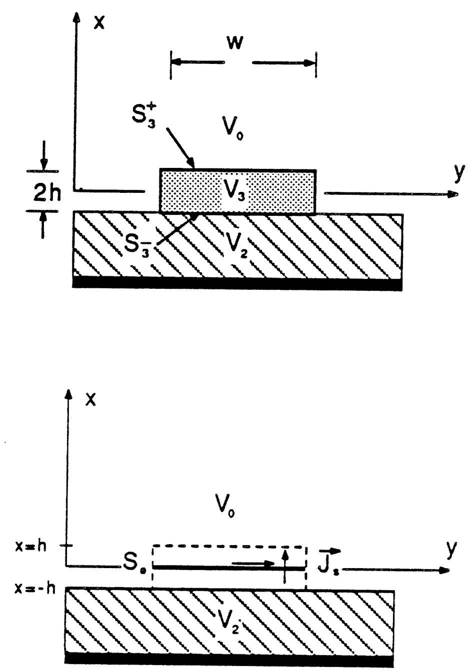

Figure 8: Equivalent polarization current.

stant of the dominant mode has been computed as a function of frequency and is shown in Figure 9. In this mode, the electric field component which is parallel to the dielectric interface (E_y) is a few orders of magnitude larger than the other two components. The theoretical results of this method show very good agreement with theoretical results derived from the classical 2-D modal analysis. As can be seen in Figure 9, the technique works very well even for electrically thick ridges ($w = 0.25\lambda_g$ at 120 GHz).

The planar integral equation technique can be further applied to study three-dimensional passive circuit elements such as power dividers, impedance transformers, bends and stubs. Such an extension is rather simple. With the replacement of the volume polarization current with an equivalent current of lower dimensionality, the original problem is simplified and can be treated as any other three-dimensional problem with unknown planar current densities. The development of this technique allows the design of novel monolithic circuits which can provide high performance at frequencies up to the terahertz region.

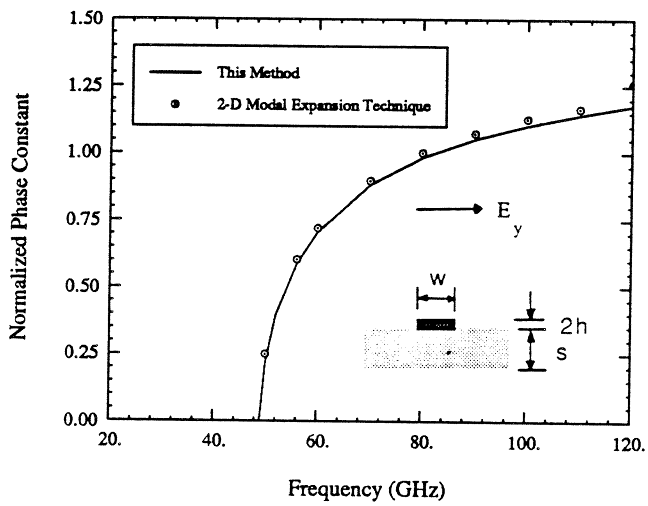

Figure 9: Comparison between the modified Green's function and the modal expansion method ($w = 0.5$ mm, $h = 62.5$ μm, $s = 250$ μm, $\epsilon_{strip} = 2$, $\epsilon_{substrate} = 12$).

5 Conclusion

Low-loss monolithic waveguides have been proposed for THz frequency applications and a modified planar integral equation approach has been developed for the analysis of monolithic structures using equivalent polarization currents. Future work in the development of these waveguides includes the optimization of the transmission lines. A wide range of designs is available; a different choice of materials, dimensions and layer arrangement could yield waveguides with better power confinement and lower losses than the examples which have been presented. In addition, three-dimensional structures will be characterized with the modified integral equation method. Experimental verification, beginning with large scale models and proceeding to actual structures, will also be performed. Eventually, the waveguides will be employed in THz monolithic circuits, such as low-loss antenna feed networks.

Acknowledgements

This work was supported by the NASA Center for Space Terahertz Technology, and by the Army Research Office under the URI program, Contract No. DAAL03-87-K-0007.

References

[1] U. Crombach, "Analysis of Single and Coupled Rectangular Dielectric Waveguides," *IEEE Trans. Microwave Theory Tech.*, vol. MTT-29, pp. 870–4, September, 1981.

[2] R. Mittra, Y. Hou and V. Jamnejad, "Analysis of Open Dielectric Waveguides Using Mode-Matching Techniques and Variational Methods," *IEEE Trans. Microwave Theory Tech.*, vol. MTT-28, pp. 36–43, January, 1980.

[3] K. Solbach and I. Wolff, "The Electromagnetic Fields and The Phase Constants of Dielectric Image Lines," *IEEE Trans. Microwave Theory Tech.*, vol. MTT-26, pp. 266–74, April, 1978.

[4] W. V. McLevige, R. Mittra, and T. Itoh, "New Waveguide Structures for Millimeter-Wave and Optical Integrated Circuits," *IEEE Trans. Microwave Theory Tech.*, vol. MTT-23, pp. 788–94, October, 1975.

[5] K. Ogusu, "Numerical Analysis of the Rectangular Dielectric Waveguide and Its Modifications," *IEEE Trans. Microwave Theory Tech.*, vol. MTT-25, pp. 874–85, November, 1977.

[6] T. Itoh, "Inverted Strip Dielectric Waveguide for Millimeter-Wave Integrated Circuits," *IEEE Trans. Microwave Theory Tech.*, vol. MTT-24, pp. 821–7, November, 1980.

[7] T. Itoh and B. Adelseck, "Trapped Image Guide for Millimeter-Wave Circuits," *IEEE Trans. Microwave Theory Tech.*, vol. MTT-28, pp. 1433–6, December, 1980.

[8] R. Mittra and S. W. Lee, *Analytical Techniques in the Theory of Guided Waves.* New York: McGraw-Hill, 1961.

[9] S. Peng and A. A. Oliner, "Guidance and Leakage Properties of a Class of Open Dielectric Waveguides: Part I—Mathematical Formulations," *IEEE Trans. Microwave Theory Tech.*, vol. MTT-29, pp. 843–55, September, 1981.

[10] A. A. Oliner and S. Peng, "Guidance and Leakage Properties of a Class of Open Dielectric Waveguides: Part II—New Physical Effects," *IEEE Trans. Microwave Theory Tech.*, vol. MTT-29, pp. 855–69, September, 1981.

[11] C. A. Balanis, *Advanced Engineering Electromagnetics.* New York: John Wiley & Sons, 1989.

[12] T. E. van Deventer, P. B. Katehi, and A. Cangellaris, "An Integral Equation Method for the Evaluation of Conductor and Dielectric Losses in High Frequency Interconnects," *IEEE Trans. Microwave Theory Tech.*, vol. MTT-37, pp. 1964–72, December, 1989.

[13] B.J. Rubin, "Full-Wave Analysis of Waveguides involving Finite-Size Dielectric Regions," *IEEE MTT-International Symposium Digest*, Dallas, pp. 705-708, May 1990.